Transmission characteristics of an excited-state induced dispersion optical filter of rubidium at 775.9 nm

Zhusong He (何竹松), Yundong Zhang (掌蕴东), Shuangqiang Liu (刘双强), and Ping Yuan (袁 萍)

State Key Laboratory of Tunable Laser Technology, Institute of Optoelectronics, Harbin Institute of Technology, Harbin 150080

Received February 7, 2007

The operation of an ultra-narrow bandwidth optical filter based on the $5P_{3/2} \rightarrow 5D_{3/2}$ excited-state transition in rubidium vapor is reported. The $5D_{3/2}$ state is excited by a circularly polarized pump beam at 780 nm from a diode laser. The filter displays a single 398-MHz bandwidth at a peak transmission of 9.0%, which is narrower than the Doppler bandwidth. The dependence of peak transmission on the pump intensity and cell temperature is also given.

OCIS codes: 120.2440, 300.6210, 300.2530, 020.4180.

With the development of laser communication and lidar[1−3], using an ultra-narrow pass-band optical filter to reject broadband background has become an important way to improve the signal-to-noise ratio (SNR) of the receiver systems. It is well known that conventional interference filters cannot provide extremely high transmission with ultra-narrow bandwidth. Laser-induced dispersion optical filter (LIDOF)[4−6] has the advantages of ultra-narrow band, high transmission, fast response, large field of view, and high noise rejecting capability. Compared with the Faraday anomalous dispersion optical filter (FADOF)[7−15], LIDOF does not need an external magnetic field and has higher transmission on excited-state transition.

In this letter, we demonstrate a LIDOF at 775.9 nm pumped by a narrow-linewidth circularly polarized light, what is to our knowledge, firstly reported in rubidium vapor. We observed a single bandwidth of 398 MHz less than Doppler band width (about 600 MHz at 410 K) with a peak transmission of 9.0%. The dependence of peak transmission on pump intensity and cell temperature is also discussed. It should be noted that the wavelengths chosen in our experiment were some kind of simulation of green-band LIDOF, for instance, Rb $5P_{1/2} \rightarrow 10S_{1/2}$ (532.24 nm), Rb $5P_{3/2} \rightarrow 11S_{1/2}$ (523.39 nm), which was a compromise due to the lack of green-band laser source. But the method is general, the results are useful for green wavelength LIDOF.

A LIDOF consists of an atomic vapor cell sandwiched between crossed polarizers and a pump laser, which provides circularly polarized light to selectively excite ground state population to the appointed magnetic sublevel of the first excited state. When linearly polarized beam travels through the dispersive atomic vapor and overlaps the pump beam, a polarization rotation occurs. The reason for polarization rotation of FADOF is the resonance enhancement and high dispersion of the Faraday effect near a narrow absorption line. In the case of LIDOF, the rotation is caused by an induced circular birefringence, which results from an induced dichroism, that is, a difference in the excited-state absorption of a left circularly polarized (LCP) and a right circularly polarized (RCP) components of the linearly polarized light. The simple three-level relevant energy diagram ($5S_{1/2} \rightarrow 5P_{3/2} \rightarrow 5D_{3/2}$) of the rubidium atom is shown in Fig. 1.

The experimental arrangement is shown schematically in Fig. 2. The rubidium vapor was generated by heating a 10-cm-long cell. The temperature was regulated by a temperature controller (Omron) with a precision of ±0.1 K. The 780-nm circularly polarized pump light used to excite the Rb atoms to the $5P_{3/2}$ state was obtained from a continuous-wave (CW) diode laser (TOPTICA DL100) and a quarter-wave retarder. A second diode laser generated the 775.9-nm linearly polarized probe beam resonant

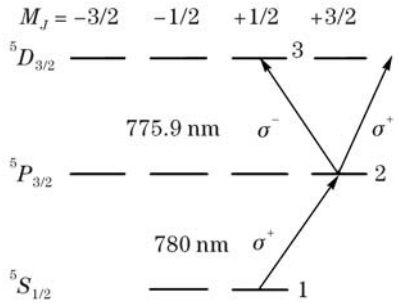

Fig. 1. Simplified relevant energy-level diagram of Rb atom. The ten-level system is truncated into a three-level system, as for reasons of ground state population transfer to excited state by circularly polarized pump light. The three levels are labeled as 1, 2, and 3 in order of increasing energy, respectively.

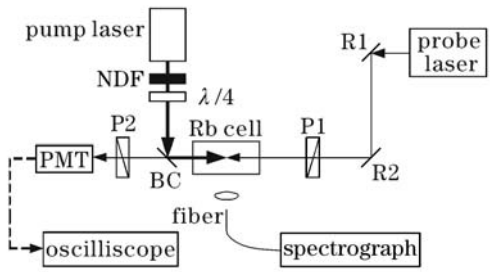

Fig. 2. Schematic diagram of the experimental setup. R1, R2: full-reflection mirrors; P1, P2: Glan-Thompson prisms; BC: beam combiner; NDF: neutral-density filters; $\lambda/4$: quarter-wave retarder.

1671-7694/2007/050252-03

with the $5P_{3/2} \rightarrow 5D_{3/2}$ transition. Both diode lasers have a nominal linewidth of 2 MHz. The beam diameters of the pump and the probe beams were 2 and 1.6 mm, respectively. Both beams were spatially overlapped over the entire length of the cell. The transmission of the probe light through the crossed polarizers when the cell was not pumped was less than 0.001%. A photomultiplier tube (PMT) was used to detect the transmitted light. An oscilloscope synchronized to the probe laser frequency recorded the output of the PMT. A spectrograph (ARC Spectro-300) was used to monitor the fluorescence.

A typical transmission spectrum of the laser-induced dispersion filter is shown in Fig. 3. It was obtained by tuning the circularly polarized pump beam with an intensity of 2.90 W/cm^2 to the $5S_{1/2} \rightarrow 5P_{3/2}$ resonance at 780 nm. With the polarizers crossed, the probe beam was scanned through the $5P_{3/2} \rightarrow 5D_{3/2}$ transition by a triangle wave current modulation with a scan range of 5 GHz. The transmitted probe intensity as a function of frequency was measured by the PMT and recorded. The measured peak transmission of 9.0% is the ratio of the maximum PMT signal to that measured with the pump beam blocked and the polarizers uncrossed. It should be noted that due to the reflected pump beam of beam combiner becomes somewhat elliptic, the peak transmission is lower than optimization value. The top trace represents the transmission spectrum of the LIDOF at 410 K. The bottom trace shows that the LIDOF transmission disappeared when the pump beam is blocked. The signal also disappears when either of the two beams is tuned off from its respective resonance.

The influence of pump intensity on the transmission is presented in Fig. 4. We measured the variation of peak transmission with pump intensity at 393, 408, and 428 K, respectively. From these results, it can be seen that peak transmission rises with the increase of pump intensity. At 393 K, peak transmission variation is almost linear. Whereas at 408 and 428 K, peak transmission places on a linear slope below 1.48 W/cm^2, but becomes saturated above 1.48 W/cm^2. The threshold occurs near the intensity where saturation causes cell to become optically thinner for the pump laser. The excited-state occupancy should not be significantly increased with the increase of pump intensity, as the pump transition is well saturated.

The peak transmission as a function of cell temperature is shown in Fig. 5. From the experimental results, it is shown that the peak transmission increases in proportion

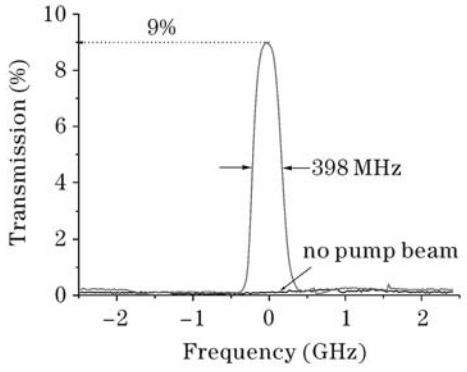

Fig. 3. Experimental transmission spectra at 775.9 nm when $I_{\rm pump} = 2.90$ W/cm^2 and $T = 410$ K in a 0.1-m-long cell.

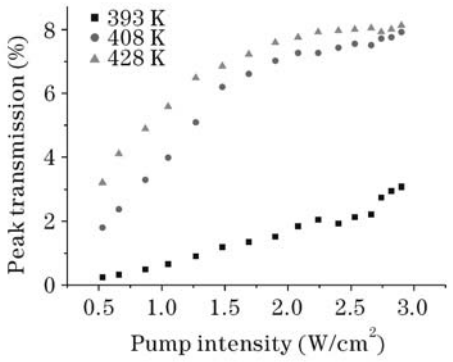

Fig. 4. Peak transmission versus pump intensity at different cell temperatures.

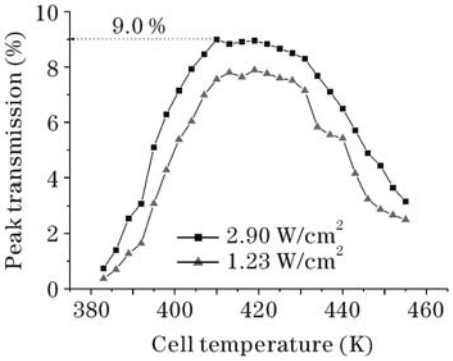

Fig. 5. Peak transmission versus cell temperature at two different pump intensities.

to the cell temperature from 383 to 410 K and reaches its optimum value near 410 K. The peak transmission varies little over the range of 410—425 K, while decreases above 425 K for the vapor becomes optically thicker for pump light at the operation intensity. The rubidium atom density rises with the increase of cell temperature, but it does not mean more excited-state population. This is due to some negative processes such as quenching and energy pooling which may surpass the pumping process when the temperature rises to a certain range.

Energy pooling places an upper limit on the vapor density of this filter, as it converts pump light at 780 nm into fluorescence, which is detected as noise. Upper states are populated by the collision $5P_{3/2} + 5P_{3/2} \rightarrow 5S + (nl = 5D, 7S) - \Delta E$[16]. The 5D product has the greatest energy pooling rate coefficients. Whereas most atoms excited to the $5D_{3/2}$ state decay by means of the $5D \rightarrow 6P \rightarrow 5S$ violet-infrared cascade which can be rejected with an additional interference filter, a few of atoms decay directly to the $5P_{3/2}$ state and emit at 775.9 nm. The energy pooling rate is proportional to the square of the density of atoms in the $5P_{3/2}$ state and hence is a sensitive function of temperature[6]. At 420 K this noise source is clearly visible as violet fluorescence. This decay process is still under investigation.

In conclusion, we have demonstrated a LIDOF pumped by a circularly polarized light in rubidium vapor. The filter displays a single peak with bandwidth of 398 MHz, which is narrower than the Doppler bandwidth (about 600 MHz at 410 K). The peak transmission as functions of pump intensity and cell temperature are shown. The

filter concept is general and may be applied to other transitions of a variety of atomic vapors.

This work was supported by the National Natural Science Foundation of China (No. 60272075 and 60478014) and partially supported by the Program of Excellent Team in Harbin Institute of Technology (HIT). We thank Professor Z. Zheng of the Department of Physics, HIT, and Associate Professor X. Yu of the Institute of Optoelectronics, HIT, for their support of some experimental apparatuses. Y. Zhang is the author to whom the correspondence should be addressed, his e-mail address is ydzhang@hit.edu.cn.

References

1. H. Chen, M. A. White, D. A. Krugger, and C. Y. She, Opt. Lett. **21,** 1093 (1996).
2. C. Fricke-Begemann, M. Alpers, and J. Höffner, Opt. Lett. **27,** 1932 (2002).
3. J. Höffner and C. Fricke-Begemann, Opt. Lett. **30,** 890 (2005).
4. S. K. Gayen, R. I. Billmers, V. M. Contarino, M. F. Squicciarini, W. J. Scharpf, G. Yang, P. R. Herczfeld, and D. M. Allocca, Opt. Lett. **20,** 1427 (1995).
5. G. Yang, R. I. Billmers, P. R. Herczfeld, and V. M. Contarino, Opt. Lett. **22,** 414 (1997).
6. L. D. Turner, V. Karaganov, P. J. O. Teubner, and R. E. Scholten, Opt. Lett. **27,** 500 (2002).
7. J. Menders, K. Benson, S. H. Bloom, C. S. Liu, and E. Korevaar, Opt. Lett. **16,** 846 (1991).
8. D. J. Dick and T. M. Shay, Opt. Lett. **16,** 867 (1991).
9. Z. Hu, X. Sun, X. Zeng, Y. Peng, J. Tang, L. Zhang, Q. Wang, and L. Zheng, Opt. Commun. **101,** 175 (1993).
10. R. I. Billmers, S. K. Gayen, M. F. Squicciarini, V. M. Contarino, W. J. Scharpf, and D. M. Allocca, Opt. Lett. **20,** 106 (1995).
11. Y. Peng, J. Phys. B **30,** 5123 (1997).
12. L. Zhang and J. Tang, Opt. Commun. **152,** 275 (1998).
13. Z. Hu and X. Zeng, Appl. Phys. Lett. **73,** 2069 (1998).
14. Y. Zhang, X. Jia, Z. Ma, and Q. Wang, IEEE. J. Quantum Electron. **37,** 372 (2001).
15. Y. Zhang, X. Jia, Z. Ma, and Q. Wang, Opt. Commun. **194,** 147 (2001).
16. Y. Shen, K. Dai, B. Mu, S. Wang, and X. Cui, Chin. Phys. Lett. **22,** 2805 (2005).